

CEAT: Continual Expansion and Absorption Transformer for Non-Exemplar Class-Incremental Learning

Xinyuan Gao¹, Songlin Dong², Yuhang He^{2*}, Xing Wei¹, Yihong Gong¹

¹School of Software Engineering, Xi'an Jiaotong University

²Institute of Artificial Intelligence and Robotics, Xi'an Jiaotong University

{gxy010317, ds1972731417}@stu.xjtu.edu.cn

heyuhang@xjtu.edu.cn, {weixing, ygong}@mail.xjtu.edu.cn

Abstract

In real-world applications, dynamic scenarios require the models to possess the capability to learn new tasks continuously without forgetting the old knowledge. Experience-Replay methods store a subset of the old images for joint training. In the scenario of more strict privacy protection, storing the old images becomes infeasible, which leads to a more severe plasticity-stability dilemma and classifier bias. To meet the above challenges, we propose a new architecture, named continual expansion and absorption transformer (CEAT). The model can learn the novel knowledge by extending the expanded-fusion layers in parallel with the frozen previous parameters. After the task ends, we losslessly absorb the extended parameters into the backbone to ensure that the number of parameters remains constant. To improve the learning ability of the model, we designed a novel prototype contrastive loss to reduce the overlap between old and new classes in the feature space. Besides, to address the classifier bias towards the new classes, we propose a novel approach to generate the pseudo-features to correct the classifier. We experiment with our methods on three standard Non-Exemplar Class-Incremental Learning (NECIL) benchmarks. Extensive experiments demonstrate that our model gets a significant improvement compared with the previous works and achieves 5.38%, 5.20%, and 4.92% improvement on CIFAR-100, TinyImageNet, and ImageNet-Subset.

1. Introduction

Class Incremental Learning (CIL) aims to recognize new classes emerging from incrementally obtained data without suffering from catastrophic forgetting [10]-performance disastrous deterioration on the previously trained data.

Some CIL methods [8, 14, 23, 26, 32] store a subset of previous exemplars in the memory buffer and replay them in the new tasks. However, in many real-world applications, the storage of previous exemplars is restricted due to privacy and security concerns. Therefore, we focus on a more practical and challenging setting of **Non-Exemplar Class Incremental Learning (NECIL)**.

Different from the general CIL setting, NECIL does not allow the model to store any old image samples and prohibits the use of any pre-trained models [17, 20, 22, 24, 33, 36, 37]. In recent works, [36] uses the augmenting prototypes of old classes to maintain the decision boundary and employ self-supervised learning to learn more generalizable and transferable features. [37] proposes a dynamic structure reorganization strategy to update the feature space and a prototype selection mechanism to reduce the feature confusion among similar classes.

Despite these methods undertaken numerous efforts to meet the challenge of NECIL, two primary challenges persist: *plasticity-stability dilemma* [1], which indicates that a model needs to be stable to maintain the old knowledge (*i.e.* stability) and be plastic to learn new one (*i.e.*, plasticity), and *classifier bias* [23], which indicates that a model's classifier is biased towards the newly emerged classes and is more likely to categorize objects into the new classes.

To address the above problems, we propose a novel architecture, named **Continual Expansion and Absorption Transformer (CEAT)** for the NECIL problem without the large-scale pre-trained model. Our approach contains two major steps, *i.e.*, parameter expansion and parameter absorption. Specifically, as shown in Fig 1, at each incremental learning task t , we construct a network with a frozen backbone to be stable of old knowledge and a set of trainable layers to be plastic for learning new ones. We expand a trainable *expanded-fusion layer (ex-fusion layer)* parallelly for some parameterized operation layer of the backbone, including convolution and linear projection in the

* Corresponding authors

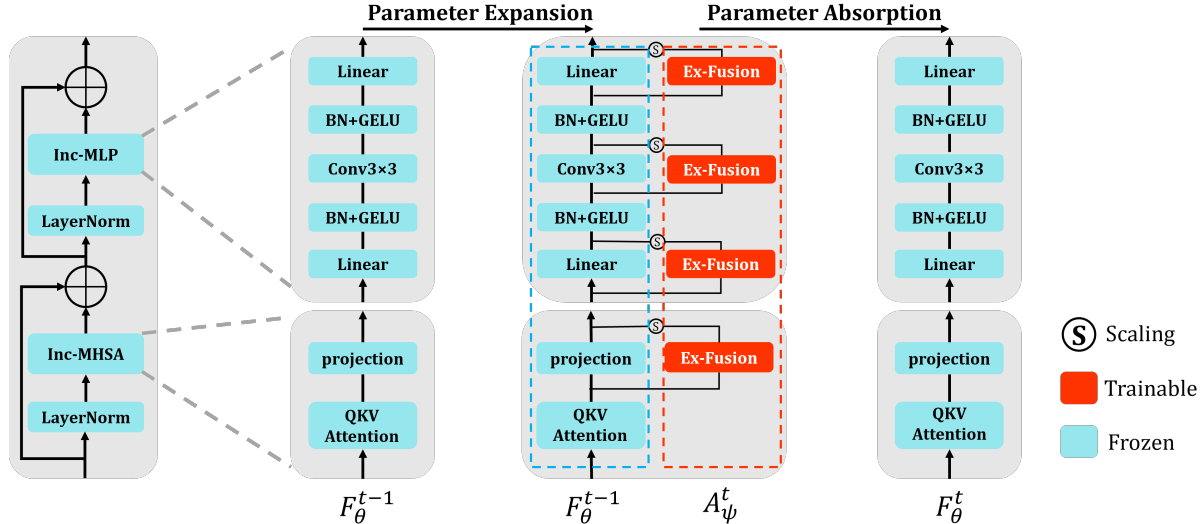


Figure 1. The overall process of our continual expansion and absorption. Each ViT layer consists of two LayerNorm layers, one incremental MHA (Inc-MHA), and one incremental MLP (Inc-MLP). In task $t > 0$, the backbone F_{θ}^{t-1} is frozen, and the ex-fusion parameters A_{ψ}^t are trainable to learn the new task. After the task ends, parameters A_{ψ}^t are absorbed losslessly into the backbone for the next task.

MLP block, and linear projection in the multi-head attention block. Only the ex-fusion layers are optimized while the original backbone is kept frozen during the training phase except for the first task. Subsequently, after the training of each session t , the optimized ex-fusion layers are *absorbed* into the backbone network by parameter-weighted summing. This remains the network structure and parameter number of the model unchanged after increment learning tasks, which is implement-friendly for practical usages and resource-constrained edge devices. To improve the ability to learn new knowledge, we propose a new loss function, named *prototype contrastive loss* (PCL), which can achieve inter-class separation and reduce the overlap between the old and new classes. Moreover, *to alleviate the classifier bias to the new classes*, we design a novel mechanism to generate the pseudo-features to correct the bias of classifiers and dynamically maintain the decision boundary of previous classes. We conduct extensive experiments on the well-established CIFAR-100, TintImageNet and ImageNet-Subset benchmarks and boast significant performance gains.

The main **contribution** of this paper is summarized as follows:

- We propose a novel ViT architecture called CEAT, to solve the NECIL problems. CEAT optimizes the ex-fusion layers while freezing the previous parameters and absorbs the expanded parameters losslessly after the task ends.
- We introduce a novel approach for generating pseudo-features that allows the model to dynamically maintain the decision boundary of previous classes.
- We develop a prototype contrastive loss to achieve

inter-class separation and reduce the overlapping among the classes.

- We conduct comprehensive experiments on three commonly used image classification benchmarks. The experimental results demonstrate that our proposed method outperforms previous approaches.

2. Related Work

Among the domains of IL, Class Incremental Learning (CIL) is a more challenging problem and has greater practical value, which has resulted in its recent surge in attention in research. Depending on whether samples need to be stored, CIL can be divided into two types: Experience-Replay CIL and Non-Exemplar CIL.

Experience-Replay Class Incremental Learning. Previous works [8, 11, 14, 23, 26, 29, 32] retain the exemplars from previous tasks in a memory buffer to replay in the new task. Current experience-replay methods can be divided into the following two classes. *Knowledge distillation methods* [7, 8, 14, 16, 23, 26] limit the output difference between the old and new networks on the data of the current task. [8, 14, 23] force the new network to reproduce similar logits to the old network to reduce forgetting. [7, 16] align the intermediate feature outputs of the old and new networks to improve the performance. [6, 26, 27] use old class data to maintain the topology structure of old feature space to alleviate forgetting. *Dynamic architecture methods* [29, 32, 35] expand extra feature extractors for each task and concatenates the feature from each feature extractor

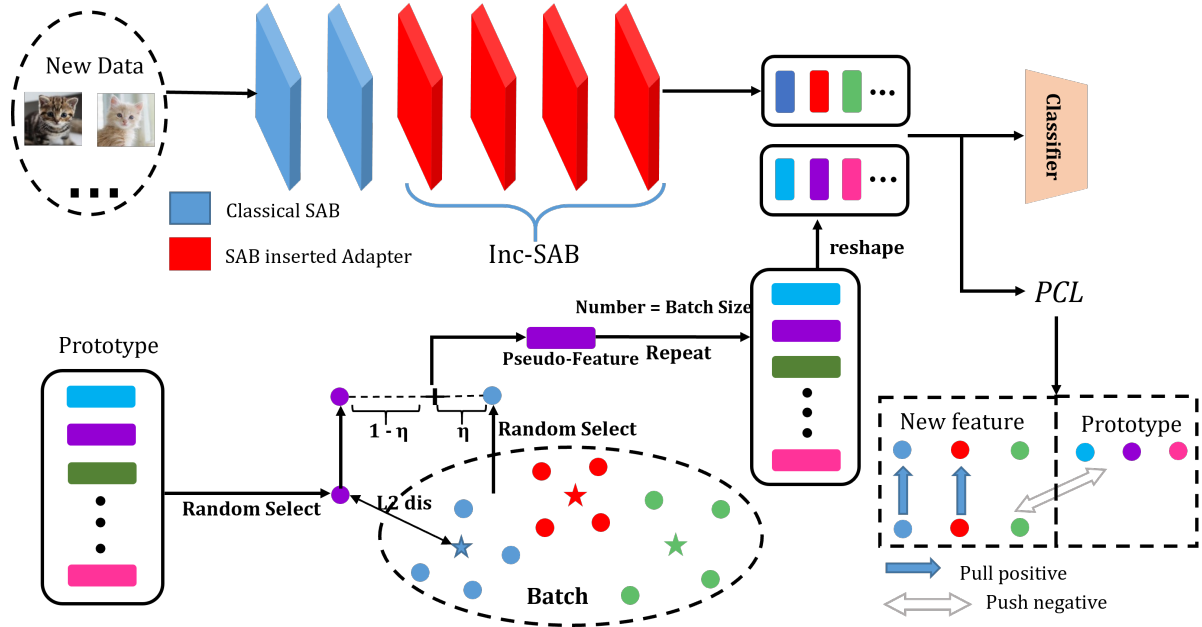


Figure 2. The overall structure of our model. Our model consists of two classical SABs (Self-Attention Blocks), four Inc-SABs, which have expanded parameters, and a classifier. The current images pass the feature extractor and the resulting features concat with the pseudo-features to balance the classifier. Also, the concat features are used to compute the PCL (prototype contrastive loss) to reduce the overlap among the old and new classes.

for classification. However these methods typically require more training memory and computing resources.

Nevertheless, on account of considerations related to privacy, security, and legal regulations, private user exemplars cannot be stored in many important scenarios of real-world applications. At the same time, storing old image samples requires a lot of additional memory overhead. These motivate us to focus on the non-exemplar setting, which is more privacy-protected.

Non-Exemplar Class Incremental Learning. Recent works [20, 24, 33, 36, 37] focus on the more challenging but more practically valuable problem of NECIL without the pre-trained model. Since NECIL does not store any old image exemplars except for a prototype per class, it encounters increased difficulty in dealing with the plasticity-stability dilemma and addressing classifier bias. Previous methods all focus on how to overcome these two problems. PASS [36] leverages augmenting prototypes of old classes to preserve the decision boundary and employs self-supervised learning to acquire more generalizable and transferable features. SSRE [37] proposes a dynamic structure reorganization strategy to update the feature space and a prototype selection mechanism to reduce the feature confusion among similar classes. FeTrIL [22] freezes the feature extractors after the first task and uses a simple pseudo-feature generator to maintain the decision boundary. These three methods

are our main comparison objects.

Class Incremental Learning in Vision Transformer.

Recent works [8, 11, 25, 30, 31] have introduced the ViT architecture into the continual learning field. [25, 30, 31] introduce the large-scale pre-trained model into the continual learning field. They freeze the pre-trained model (ViT B16 pre-trained on ImageNet21K) as the backbone and optimize the prompts to tune the model for the downstream tasks. L2P [31] proposes a key-query matching strategy to select the prompts from the prompt pool, and then insert them into the pre-trained model. CODA [25] weighting the prompts and can be optimized in an end-to-end fashion. However, These methods heavily depend on a large-scale pre-trained model. Thus these methods are difficult to deploy in resource-constrained edge devices due to the large pre-trained model. Moreover, when facing a new dataset that has a significant distance from the pre-trained data, these methods often perform satisfactorily. *In this paper, we do not compare with such methods because their performance declines disastrously without the large-scale pre-trained model.*

Some methods [8, 11, 15] are experience-replay methods without the pre-trained model. DyTox [8] and DKT [11] design various tokens to retain the information from previous tasks and use the old samples to correct the classifier bias. DNE [15] propose a network-expanded method to reduce

the forgetting and balance the trade-off between accuracy and model size.

However, [34] have showcased that ViTs suffer from more serious forgetting when trained from scratch. Thus applying ViT architecture to the NECIL problem is still lacking research. To meet this challenge, we attempt to propose a novel architecture based on the vision transformer, which has a similar parameter amount to previous works and can be trained from scratch, for the NECIL problem.

3. Methodology

3.1. Problem Setting

Given a dataset $D = \{D_t\}_{t=0}^T$ of T incremental learning sessions, where D_0 is used to train a base model and D_t ($t > 0$) is used for incremental learning. Each element $D_t = \{X_t, Z_t\}$ of D is composed of a training set X_t and a testing set Z_t . For each training set $X_t = \{(x_t^i, y_t^i)\}_{i=1}^{N_t}$, x_t^i denotes the i -th sample, $y_t^i \in C_t$ denotes the class label, where C_t denotes the label set of the t -th session. The objective of NECIL is to incrementally train a unified DNN model across the T sessions without requiring storing old class samples during the learning process. Specifically, at each session t , only X_t is available for training, and the model is evaluated on a combined testing set $Z_{0 \sim t} = Z_0 \cup \dots \cup Z_t$ and is required to recognize all the old classes encountered $C_{0 \sim t} = C_0 \cup \dots \cup C_t$.

3.2. Continual Expansion and Absorption

For simplicity, we define the feature extractor as $F^t(\cdot, \theta)$, the classifier as $g(\cdot, \phi)$, and the ex-fusion layer as $A^t(\cdot, \psi)$, where t is the task id. For the first phase, we optimize the model F_θ^0 on dataset D_0 . After the first phase, we repeatedly execute our expansion and absorption operation for incremental learning.

Parameter Expansion. At each task t , we first freeze the feature extractor F_θ^{t-1} from the previous task to maintain the stability of the model. The classifier g_ϕ^{t-1} extends the head to g_ϕ^t , which is trainable, to accommodate the increase of categories. To learn the new task, we define a series of trainable parameters of ex-fusion layer $A_\psi^t = A_{\psi_1}^t \dots A_{\psi_i}^t$, where i is the index of the ex-fusion layer. To adhere to the principles of simplicity and effectiveness, the ex-fusion layer is defined solely as a bias-free linear layer

$$A_{\psi_i}^t(x_i) = \psi_i * x_i \quad (1)$$

where ψ_i is the weight parameters of the ex-fusion layer and x_i is the input feature map.

During the incremental training phase, the A_ψ^t are extended in parallel with the different frozen backbone module $F_{\theta_1}^{t-1} \dots F_{\theta_i}^{t-1}$. We optimize the A_ψ^t to force the model

to learn new knowledge. The input feature map x_i is fed into the expanded layer and the backbone module respectively. Then the results are summed into a new feature map to the next layer

$$x_{i+1} = F_{\theta_i}^{t-1}(x_i) + \lambda * A_{\psi_i}^t(x_i) \quad (2)$$

where λ is the scaling parameter in different incremental scenarios. $\lambda = Num(C_t)/10$, where $Num(C_t)$ is the number of C_t . The following λ has the same meaning as this equation.

Parameters Absorption. To avoid the continuous augmentation in both memory usage and the number of parameters, we absorb the extended parameters A_ψ^t into the main backbone F_θ^{t-1} to form a new backbone upon task completion

$$F_\theta^t = F_\theta^{t-1} + \lambda * A_\psi^t \quad (3)$$

After completion of task t , all the expanded parameters A_ψ^t are absorbed losslessly into the main backbone to maintain a constant total parameter amount. This significantly enhances the practicality of our model in different incremental scenarios.

Absorption implementation. The classical vision transformer model have three typical trainable modules in each block: the MHSA (Multi-Head Self-Attention) module, the linear layer, and the convolutional layer. To highlight the comprehensive consideration, we discuss the implementation of lossless absorption in the above three modules, respectively.

For the MHSA module, which consists of a QKV-Attention and a projection layer. We opt to expand the parameters in parallel with the projection layer to enable dynamic adaptation, instead of the QKV-Attention. The reason is that despite the QKV-Attention module varies across different ViT blocks, all of them possess a projection layer in the MHSA. Without loss of generality, we show the MHSA of l -th layer. The detail is as follows:

$$\begin{aligned} x_a &= \text{Softmax}\left(\frac{Q_l \cdot K_l^T}{\sqrt{d}}\right) V_l, \\ x_{l1} &= \text{Proj}(x_a), \quad x_{l2} = \lambda \cdot A_\psi(x_a), \\ x_l &= x_{l1} + x_{l2}. \end{aligned} \quad (4)$$

where $Proj$ represents a projection layer and Q_l . K_l , V_l represents the standard QKV operations in the vision transformer.

After the training phase, since the projection layer is essentially a linear layer, the lossless absorption is equivalent to the absorption of the linear layer in the following.

For the linear layer, we can simply sum the two linear layer weights to fuse two linear layers into a single linear layer

$$W_{new} = W_{linear} + \lambda * \psi, \quad (5)$$

where W_{linear} is the linear layer weight in the main backbone and W_{new} is the linear weight after absorption.

As both the 1×1 convolution and linear layers are consistent in structure and function, it is easy to implement by zero-padding the 1×1 kernel to 3×3 and adding the two kernels up

$$\begin{aligned} W_{3*3} &= ZP(\psi), \\ W_{new} &= W_1 + \lambda * W_{3*3} \end{aligned} \quad (6)$$

where ZP represents the zero-padding operation, W_1 represents the 3×3 convolution in the main backbone.

3.3. Batch Interpolation Pseudo-Features

Prototype. Due to the risks of data leakage and privacy violations, the NECIL problem does not permit the storage of any past samples except for one prototype per class. Following the recent research, we calculate the class center vector for each class and maintain it as the prototype

$$P_{t,k} = \frac{1}{N_{t,k}} \sum_{n=1}^{N_{t,k}} F_{\theta}(x_k^t) \quad (7)$$

where t is a new task, x_k^t is an image of class k in task t , and $N_{t,k}$ is the number of training images of class k . We set the prototypes $P = \{P_1, \dots, P_i, \dots\}$. The number of prototypes is equal to the number of old classes.

To preserve the decision boundaries and correct the classifier, we propose batch interpolation to generate pseudo-features. Consistent with recent research, we only generate an equal number of pseudo-features for each batch to ensure a fair comparison.

Feature Select. Firstly We calculate the class center of each new class in the batch. We define the class center $S = \{S_1, \dots, S_j, \dots\}$ in the batch of new training data

$$S_j = \frac{1}{M_{t,j}} \sum_{i=1}^{M_{t,j}} F_{\theta}(x_j^t) \quad (8)$$

where M is the number of features of this class in the batch. Then we randomly select a prototype P_i to generate the pseudo-features. We compute the distance between P_i and S in the feature space by L2 distance and select the nearest class center from S .

Interpolation. We assume that the nearest class center vector is S_j , which belongs to the class j . We use interpolation to generate the pseudo-features to maintain the decision boundary. without loss of robustness, we randomly

select a feature that belongs to the class j , named F_j . We use a similar approach to interpolation

$$F_{ipf} = (1 - \eta)P_i + \eta F_j \quad (9)$$

the F_{ipf} has the same label as P_k . η is a hyperparameter to control the position of the pseudo feature. The $\eta \sim \zeta * Beta(0.8, 0.5)$, where ζ increases linearly with tasks from 0.5 to 0.7.

The benefit of using interpolation to generate the pseudo-features is two-fold. Firstly, the pseudo feature is generated by the nearest class and the prototype. Hence the decision boundary of the old classes is flexible, which leads to a better pseudo-feature distribution. Secondly, the pseudo-features mix information from old and new classes and dynamically adjust with the batch. Therefore, batch interpolation pseudo-feature effectively solves the problem that the decision boundary maintained by Gaussian noise gradually loses efficacy as tasks increase. As the feature space keeps changing, the decision boundaries can still effectively distinguish the old and new classes.

3.4. Prototype Contrastive Loss

Previous methods usually ignore the importance of inter-class separation in the NECIL problem. To tackle the problem and enhance the ability to learn, we propose a prototype contrastive loss (PCL) scheme. Under the unavailability of old class data, prototype contrastive learning achieves inter-class separation and reduces the overlap between old and new classes.

During the t -th training phase, our model stores a series of frozen prototypes $P = \{P_1, \dots, P_i, \dots\}$. The feature extractor F_{θ} projects an image x to a feature $z = F_{\theta}(x)$. The classifier g_{ϕ} projects the feature z to a vector $\hat{y} = g_{\phi}(z)$. Without training the g_{ϕ} , given a batch of training images $B = \{(x_i, y_i)\}_{i=1}^N$. The feature map is trained to minimize the prototype contrastive loss

$$\begin{aligned} L_{pcl} &= \sum_{i \in B} \frac{-1}{|p_i|} \sum_{p \in p_i} \log \left(\frac{\exp(z_i \cdot z_p / \tau)}{\sum_{z_j \in A(i)} \exp(z_i \cdot z_j / \tau)} \right) \\ &+ \sum_{i \in B \cup P} \frac{-1}{|p_i|} \sum_{p \in p_i} \log \left(\frac{\exp(z_i \cdot z_p / \tau)}{\sum_{z_j \in A(i) \cup P} \exp(z_i \cdot z_j / \tau)} \right) \end{aligned} \quad (10)$$

where τ is a temperature hyperparameter; $A(i)$ is the set of the feature in the augmented batch B . $p_i = \{p \in A(i) : \hat{y}_p = \hat{y}_i\}$ is the index set of positive samples, which have the same label.

The prototypes serve as an anchor to force new class features away from the feature distribution of old classes to maintain the distribution. Moreover, the PCL achieves inter-class separation between old and new classes instead of the mere separation among new classes in the previous

contrastive loss. This improvement alleviates the confusion between old and new classes, which enhances the learning ability of new classes without forgetting more old knowledge. The ablation experiments demonstrate the effectiveness of prototype contrastive loss.

3.5. Optimization Objective

As the ex-fusion layers continuously modify the feature space of the model, we require distillation to constrain the changes made to the feature space. Following the previous works, we employ the knowledge distillation (KD) [13], including the logit distillation L_{ld} and feature distillation L_{fd} , to constrain the feature extractor

$$L_{kd} = L_{ld} + L_{fd} \quad (11)$$

where L_{fd} uses the L_1 distance. By combining the prototype contrastive loss L_{pcl} and interpolation pseudo-feature loss L_{ipf} that we proposed above, we can obtain the comprehensive loss function L_{total}

$$L_{total} = L_{bce} + \alpha L_{kd} + \mu L_{ipf} + \delta L_{pcl} \quad (12)$$

where L_{bce} is used to train the new classes. δ , α , and μ are the hyperparameters. δ is set to 0.5. We set $\alpha = Num(C_{1:t})/Num(C_t)$ as done by previous work [8, 11], and $\mu = Num(C_{1:t})/20$, which removes the need to finely tune this hyperparameter in different datasets. The details are added in the Appendix.

4. Experiment

4.1. Experimental Settings

Datasets. We use three common image classification benchmarks: CIFAR100 [18], TinyImageNet [19] and ImageNet-Subset [4] following recent work [22, 36, 37]. CIFAR-100 [18] contains 100 classes, each class containing 500 training images and 100 test images. Each image is represented by 32×32 pixels, which is particularly small for ViT architecture. Tiny-ImageNet has 200 classes, each class containing 500 training images, 50 testing images, and 50 validation images. Each image is represented by 64×64 . ImageNet-Subset is a 100-class subset of ImageNet [5]. ImageNet-Subset contains about 130000 images for training and 50 images per class for testing. Each image is represented by 224×224 .

Experimental Setup. We design three standard NECIL settings like previous works [22, 36, 37] to validate the incremental performance of our model. For CIFAR100, we set 50 classes as the base training data and increased 5/10 classes per task. We also set 40 classes as the base training data and increased 3 classes per task to test long-range increment learning ability. For TinyImageNet, we set

100 classes as the base training data and increased 5/10/20 classes per task. For ImageNet-Subset, we set 50 classes as the base training data and increased 5 classes per task. The random seed is 1993 following the previous work.

Evaluation Metric. Following the [22, 36, 37], we employed the average incremental accuracy [23] and average forgetting [3] as the main evaluation metric. The average incremental accuracy is calculated by averaging the accuracy of each task, serving as a crucial metric for assessing overall incremental performance. The average forgetting is calculated on average by the difference between the accuracy rate after each task and the final accuracy rate, representing the model’s ability to mitigate catastrophic forgetting.

Implementation Details. The ViT-based feature extractor $F(\cdot, \theta)$ of our model consists of six SABs like DyTox [8] to satisfy the limit of parameters in the NECIL problem. To compare with other methods that use ResNet18 [12] as the backbone fairly, the final number of parameters of our model is 10.89M in CIFAR100 and 11.10M in ImageNet-Subset, slightly less than ResNet18 (11.22M). More training information will be provided in the Appendix.

4.2. Main Properties and Analysis

Average Accuracy. We compare our method with other methods based on the average accuracy and report it in Table 1. The experimental results indicate that our method achieves significantly better performance compared to the previous NECIL method [22, 37]. In CIFAR100, our method surpasses the second-best by up to **5.38%**, **4.26%**, and **3.44%**, which demonstrates the ability to adapt the transformer architecture to the NECIL problem on small datasets. In TinyImageNet and ImageNet-Subset, our method surpasses the second best by up to **5.19%**, **5.20%**, and **3.79%** on TinyImageNet and **4.92%** on ImageNet-Subset. Moreover, It is worth noting that our method exhibits remarkable improvements over the classical example-based approaches, further alleviating the dependence of incremental learning on examples.

Average Forgetting. We report the average forgetting of different methods in Table 2. Compared to other state-of-the-art methods [22, 36, 37], our approach demonstrates a notable advantage in terms of average forgetting across CIFAR-100 and TinyImageNet.

Visualization. To further illustrate the effectiveness of our approach, we show the visualization result with t-SNE [28]. After the final task ends, we freeze the final model and use the previous images from the first 10 classes to compute

Methods	Buffer size	CIFAR-100			TinyImageNet			ImageNet-Subset
		$P=5$	$P=10$	$P=20$	$P=5$	$P=10$	$P=20$	$P=10$
iCaRL-CNN [23]	20/class	51.07	48.66	44.43	34.64	31.15	27.90	50.53
iCaRL-NCM [23]		58.56	54.19	50.51	45.86	43.29	38.04	60.79
EEIL [2]		60.37	56.05	52.34	47.12	45.01	40.50	63.34
UCIR [14]		63.78	62.39	59.07	49.15	48.52	42.83	66.16
DyTox-ViT [8]		69.84	67.68	63.23	58.16	57.69	54.74	74.43
EWC [17]	0/class	24.48	21.20	15.89	18.80	15.77	12.39	20.40
LwF [20]		45.93	27.43	20.07	29.12	23.10	17.43	31.18
MUC [21]		49.42	30.19	21.27	32.58	26.61	21.95	35.07
SDC [33]		56.77	57.00	58.90	-	-	-	61.12
PASS [36]		63.47	61.84	58.09	49.55	47.29	42.07	61.80
SSRE [37]		65.88	65.04	61.70	50.39	48.93	48.17	67.69
FeTrIL [22]		66.30	65.20	61.50	54.80	53.10	52.20	71.20
CEAT		71.68+5.38	69.46+4.26	65.14+3.44	59.89+5.19	58.30+5.20	55.89+3.79	76.12+4.92

Table 1. Comparisons of the average incremental accuracy (%) at different settings on CIFAR-100, TinyImageNet, ImageNet-Subset. P represents the number of phases, and buffer size represents the number of exemplars. The results are obtained from SSRE [37] and FeTrIL [22]. We reproduced the ViT-based method DyTox [8] of experience-replay CIL for further comparison. The improvement compared to the SOTA results is in the last row.

Methods	CIFAR-100			TinyImageNet		
	5	10	20	5	10	20
iCaRL-CNN [23]	42.13	45.69	43.54	36.89	36.70	45.12
iCaRL-NCM [23]	24.90	28.32	35.53	27.15	28.89	37.40
EEIL [2]	23.36	26.65	32.40	25.56	25.91	35.04
UCIR [14]	21.00	25.12	28.65	20.61	22.25	33.74
LwF_MC [20]	44.23	50.47	55.46	54.26	54.37	63.54
MUC [21]	40.28	47.56	52.65	51.46	50.21	58.00
PASS [36]	25.20	30.25	30.61	18.04	23.11	30.55
SSRE [37]	18.37	19.48	19.00	9.17	14.06	14.20
FeTrIL [22]	14.46	15.31	17.08	8.02	10.23	10.64
CEAT	7.85	8.04	8.68	6.10	5.21	6.01

Table 2. Results of average forgetting on 5, 10 and 20 phases in CIFAR100 and TinyImageNet. The results are obtained from [37]. Average forgetting demonstrates its ability to reduce catastrophic forgetting.

the feature space distribution of these classes. The distribution of different classes is better distinguished, which means the anti-forgetting effect is better. We report the result in figure 3. It is worth noting that the final model of our method can still distinguish the features of the first 10 classes well compared with previous methods [22, 36]. This corresponds to our great anti-forgetting results in average forgetting.

4.3. Discussion on Motivation and Comparison

Additional Motivation. As we mentioned in related work, [34] have showcased that ViTs are more prone to forgetting when trained from scratch. Therefore, we have conducted the experiment to verify whether the previous method is suitable for the ViT structure. We reproduce the most representative method-PASS [36] with the same ViT

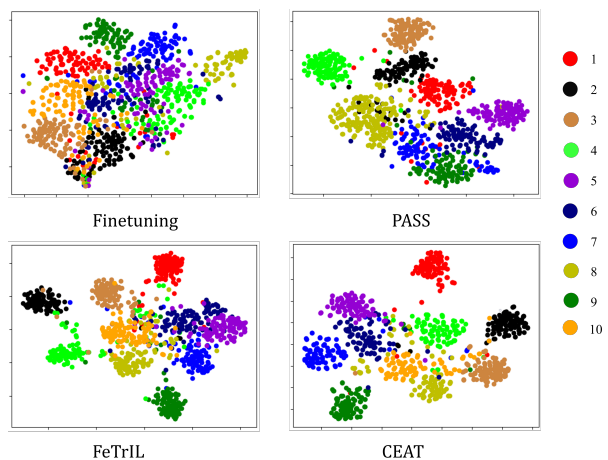


Figure 3. The visualization of the old feature using the final model on CIFAR-100 5 steps. We utilize the preceding images from the first 10 categories to evaluate the capability of the final model in preserving the distinguishing features of initial class categories.

Methods	Params	CIFAR-100		
		$P=20$	$P=10$	$P=5$
PASS-CNN	11.22M	58.09	61.84	63.47
PASS-ViT	10.89M	43.21	55.04	59.78
CEAT-ViT	10.89M	65.14	69.46	71.68

Table 3. We reproduce PASS with the same ViT backbone, data augmentation, and hyperparameter tuning as our method on CIFAR-100. It is worth noticing that despite the adjustment of hyperparameters, PASS still performs disastrously based on ViT architecture, especially long-range increment learning.

backbone and data augmentation as our method. We tune all additional hyperparameters using 20% of the training data as validation data like our model to reach a better performance. We report the results in table 3. It is worth noticing that despite the large adjustment of hyperparameters, the previous method still performs disastrously, especially the longer sequences of incremental training sessions. This motivates us to propose a new approach to apply the ViT architecture to the NECIL problem.

Comparison Analysis. For a fair comparison, we compare our method with previous methods from multiple aspects. **Firstly**, in order to meet the limitation on the parameters of the NECIL problem, the final number of parameters of our model is 10.89M in CIFAR100 and 11.10M in ImageNet-Subset, slightly less than ResNet18 (11.22M) to ensure the fairness of the comparison. **Secondly**, we report the line graphs in figure 4. It is worth noting that our method has a similar initial performance to other state-of-the-art methods and gets a better last accuracy. This phenomenon corresponds to our average forgetting result reported in the main text. **Lastly**, we report accuracy of other ViT-based general CIL method [9], which stores 20 images per class in memory buffer. Our method still exhibits comparable performance, which shows that our method effectively fills the performance gap caused by the storage of examples, highlighting its practicality and effectiveness.

The above phenomena prove that our model can effectively apply ViT architecture to NECIL problems and reach a comparable performance with other ViT-based general CIL methods. The ablation study demonstrates how our contributions improve the model step-by-step.

4.4. Ablation Analyses

Contribution Ablation Analyses. We show the contribution ablation result in table 4. We established a baseline model consisting of six SABs and the Gaussian noise pseudo-features. **The baseline is the standard PASS model, which replaces ResNet18 with ViT.** To demonstrate the efficacy of our proposed approach, we incrementally incorporated components of Freeze, Batch Interpolation Pseudo-Features (IPF), Continual Expansion and Absorption (CEA), and Prototype Contrastive Loss (PCL) into the baseline model. We conduct the experiments on three incremental settings of the CIFAR100 dataset. Firstly, we freeze the backbone and tune the classifier with new data. Secondly, we replace Gaussian noise pseudo-features with our IPF, which has improved the performance significantly under the three settings. This result shows that the IPF effectively solves the problem of decision boundary degradation in previous work. In addition, The CEA expands the ex-fusion to learn new knowledge continuously while maintaining the previous parameters frozen, which makes

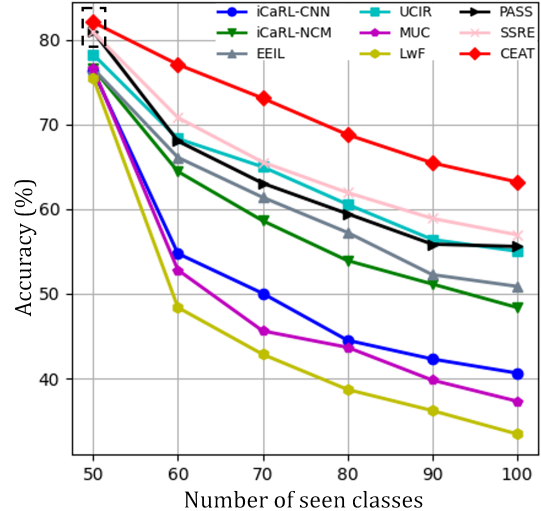


Figure 4. The performance on CIFAR-100 5 steps. Note that at the first step before the continual process begins (represented by a dotted rectangle), our model has performance comparable to other last methods [36,37]. This phenomenon illustrates that our method improves performance by solving the plasticity-stability dilemma.

impressive progress in different settings. The PCL enforces the separation of new and old classes and improves the learning of new classes. It’s worth noting that the improvement of PCL in three settings is various. The more new classes that need to be learned in each phase, the more obvious the improvement of PCL becomes. This phenomenon may be caused that the model can learn well when facing fewer new classes so that the effect of PCL is not obvious. More ablation analyses about the inserted layer and inserted position are added in the Appendix.

Freeze	IPF	CEA	PCL	CIFAR-100		
				20 phases	10 phases	5 phases
×	×	×	×	43.21	55.04	59.78
✓	×	×	×	46.71	56.21	62.95
✓	✓	×	×	50.99	61.15	65.06
✓	✓	✓	×	65.10	68.80	69.49
✓	✓	✓	✓	65.14	69.46	71.68

Table 4. Ablation study of our method on CIFAR-100 with different settings. We gradually add our contributions to the baseline model to prove its effectiveness.

5. Conclusion

The objective of CIL is to continually acquire new classes while preventing the degradation of previously learned classes when they are not accessible. Experience-replay methods are to store a set of old samples to replay, which poses privacy and data leakage risks in the real world. To solve these problems, researchers propose the NECIL,

which does not allow the model to store any old samples and does not use the pre-trained model. However, its performance is inferior to experience-replay methods due to the lack of old images. For these phenomena, our paper proposes a continual expansion and absorption transformer (CEAT), which meets the main challenges in NECIL and reaches state-of-the-art performance. Based on the unique ViT architecture, we employ ex-fusion layers to enable the learning of new knowledge while preserving previously acquired knowledge by fixing the main backbone. In order to improve the learning ability of new classes, we propose a Prototype Contrastive Loss to reduce the overlap of new and old classes. Moreover, to address the issue of classifier bias, we introduce a new batch interpolation pseudo-features approach. The ablation study provides further evidence of the efficacy of the proposed methods.

References

- [1] Gail A Carpenter and Stephen Grossberg. A massively parallel architecture for a self-organizing neural pattern recognition machine. *Computer vision, graphics, and image processing*, 37(1):54–115, 1987. [1](#)
- [2] Francisco M Castro, Manuel J Marín-Jiménez, Nicolás Guil, Cordelia Schmid, and Karteek Alahari. End-to-end incremental learning. In *ECCV*, pages 233–248, 2018. [7](#)
- [3] Arslan Chaudhry, Puneet K Dokania, Thalaiyasingam Ajanthan, and Philip HS Torr. Riemannian walk for incremental learning: Understanding forgetting and intransigence. In *Proceedings of the European conference on computer vision (ECCV)*, pages 532–547, 2018. [6](#)
- [4] Jia Deng, Wei Dong, Richard Socher, Li-Jia Li, Kai Li, and Li Fei-Fei. Imagenet: A large-scale hierarchical image database. In *2009 IEEE conference on computer vision and pattern recognition*, pages 248–255. Ieee, 2009. [6](#)
- [5] Jia Deng, Wei Dong, R. Socher, Li Jia Li, Kai Li, and Fei Fei Li. Imagenet: A large-scale hierarchical image database. In *CVPR*, pages 248–255, 2009. [6](#)
- [6] Songlin Dong, Xiaopeng Hong, Xiaoyu Tao, Xinyuan Chang, Xing Wei, and Yihong Gong. Few-shot class-incremental learning via relation knowledge distillation. In *Proceedings of the AAAI Conference on Artificial Intelligence*, volume 35, pages 1255–1263, 2021. [2](#)
- [7] Arthur Douillard, Matthieu Cord, Charles Ollion, Thomas Robert, and Eduardo Valle. Podnet: Pooled outputs distillation for small-tasks incremental learning. In *European Conference on Computer Vision*, pages 86–102. Springer, 2020. [2](#)
- [8] Arthur Douillard, Alexandre Ramé, Guillaume Couairon, and Matthieu Cord. Dytox: Transformers for continual learning with dynamic token expansion. In *Proceedings of the IEEE/CVF Conference on Computer Vision and Pattern Recognition*, pages 9285–9295, 2022. [1](#), [2](#), [3](#), [6](#), [7](#)
- [9] Arthur Douillard, Alexandre Ramé, Guillaume Couairon, and Matthieu Cord. Dytox: Transformers for continual learning with dynamic token expansion. In *Proceedings of the IEEE/CVF Conference on Computer Vision and Pattern Recognition*, pages 9285–9295, 2022. [8](#)
- [10] Robert M French. Catastrophic forgetting in connectionist networks. *Trends in cognitive sciences*, 3(4):128–135, 1999. [1](#)
- [11] Xinyuan Gao, Yuhang He, Songlin Dong, Jie Cheng, Xing Wei, and Yihong Gong. Dkt: Diverse knowledge transfer transformer for class incremental learning. In *Proceedings of the IEEE/CVF Conference on Computer Vision and Pattern Recognition*, pages 24236–24245, 2023. [2](#), [3](#), [6](#)
- [12] Kaiming He, Xiangyu Zhang, Shaoqing Ren, and Jian Sun. Deep residual learning for image recognition. In *Proceedings of the IEEE conference on computer vision and pattern recognition*, pages 770–778, 2016. [6](#)
- [13] Geoffrey Hinton, Oriol Vinyals, and Jeff Dean. Distilling the knowledge in a neural network. *Computer Science*, 14(7):38–39, 2015. [6](#)
- [14] Saihui Hou, Xinyu Pan, Chen Change Loy, Zilei Wang, and Dahua Lin. Learning a unified classifier incrementally via re-balancing. In *Proceedings of the IEEE Conference on Computer Vision and Pattern Recognition*, pages 831–839, 2019. [1](#), [2](#), [7](#)
- [15] Zhiyuan Hu, Yunsheng Li, Jiancheng Lyu, Dashan Gao, and Nuno Vasconcelos. Dense network expansion for class incremental learning. In *Proceedings of the IEEE/CVF Conference on Computer Vision and Pattern Recognition*, pages 11858–11867, 2023. [3](#)
- [16] Minsoo Kang, Jaeyoo Park, and Bohyung Han. Class-incremental learning by knowledge distillation with adaptive feature consolidation. In *Proceedings of the IEEE/CVF conference on computer vision and pattern recognition*, pages 16071–16080, 2022. [2](#)
- [17] James Kirkpatrick, Razvan Pascanu, Neil Rabinowitz, Joel Veness, Guillaume Desjardins, Andrei A Rusu, Kieran Milan, John Quan, Tiago Ramalho, Agnieszka Grabska-Barwinska, et al. Overcoming catastrophic forgetting in neural networks. *Proceedings of the national academy of sciences*, 114(13):3521–3526, 2017. [1](#), [7](#)
- [18] Alex Krizhevsky and Geoffrey Hinton. Learning multiple layers of features from tiny images. Technical report, Cite-seer, 2009. [6](#)
- [19] Ya Le and Xuan Yang. Tiny imagenet visual recognition challenge. *CS 231N*, 7(7):3, 2015. [6](#)
- [20] Zhizhong Li and Derek Hoiem. Learning without forgetting. *T-PAMI*, 40(12):2935–2947, 2018. [1](#), [3](#), [7](#)
- [21] Yu Liu, Sarah Parisot, Gregory Slabaugh, Xu Jia, Ales Leonardis, and Tinne Tuytelaars. More classifiers, less forgetting: A generic multi-classifier paradigm for incremental learning. In *Computer Vision—ECCV 2020: 16th European Conference, Glasgow, UK, August 23–28, 2020, Proceedings, Part XXVI 16*, pages 699–716. Springer, 2020. [7](#)
- [22] Grégoire Petit, Adrian Popescu, Hugo Schindler, David Picard, and Bertrand Delezoide. Fetrl: Feature translation for exemplar-free class-incremental learning. In *Proceedings of the IEEE/CVF Winter Conference on Applications of Computer Vision*, pages 3911–3920, 2023. [1](#), [3](#), [6](#), [7](#)

- [23] Sylvestre-Alvise Rebuffi, Alexander Kolesnikov, Georg Sperl, and Christoph H Lampert. icarl: Incremental classifier and representation learning. In *CVPR*, pages 2001–2010, 2017. [1](#), [2](#), [6](#), [7](#)
- [24] Wuxuan Shi and Mang Ye. Prototype reminiscence and augmented asymmetric knowledge aggregation for non-exemplar class-incremental learning. In *Proceedings of the IEEE/CVF International Conference on Computer Vision*, pages 1772–1781, 2023. [1](#), [3](#)
- [25] James Seale Smith, Leonid Karlinsky, Vyshnavi Gutta, Paola Cascante-Bonilla, Donghyun Kim, Assaf Arbel, Rameswar Panda, Rogerio Feris, and Zsolt Kira. Coda-prompt: Continual decomposed attention-based prompting for rehearsal-free continual learning. In *Proceedings of the IEEE/CVF Conference on Computer Vision and Pattern Recognition*, pages 11909–11919, 2023. [3](#)
- [26] Xiaoyu Tao, Xinyuan Chang, Xiaopeng Hong, Xing Wei, and Yihong Gong. Topology-preserving class-incremental learning. In *European Conference on Computer Vision*, pages 254–270. Springer, 2020. [1](#), [2](#)
- [27] Xiaoyu Tao, Xiaopeng Hong, Xinyuan Chang, Songlin Dong, Xing Wei, and Yihong Gong. Few-shot class-incremental learning. In *Proceedings of the IEEE/CVF Conference on Computer Vision and Pattern Recognition*, pages 12183–12192, 2020. [2](#)
- [28] Laurens Van der Maaten and Geoffrey Hinton. Visualizing data using t-sne. *Journal of machine learning research*, 9(11), 2008. [6](#)
- [29] Fu-Yun Wang, Da-Wei Zhou, Han-Jia Ye, and De-Chuan Zhan. Foster: Feature boosting and compression for class-incremental learning. *arXiv preprint arXiv:2204.04662*, 2022. [2](#)
- [30] Zifeng Wang, Zizhao Zhang, Sayna Ebrahimi, Ruoxi Sun, Han Zhang, Chen-Yu Lee, Xiaoqi Ren, Guolong Su, Vincent Perot, Jennifer Dy, et al. Dualprompt: Complementary prompting for rehearsal-free continual learning. *arXiv preprint arXiv:2204.04799*, 2022. [3](#)
- [31] Zifeng Wang, Zizhao Zhang, Chen-Yu Lee, Han Zhang, Ruoxi Sun, Xiaoqi Ren, Guolong Su, Vincent Perot, Jennifer Dy, and Tomas Pfister. Learning to prompt for continual learning. In *Proceedings of the IEEE/CVF Conference on Computer Vision and Pattern Recognition*, pages 139–149, 2022. [3](#)
- [32] Shipeng Yan, Jiangwei Xie, and Xuming He. Der: Dynamically expandable representation for class incremental learning. In *Proceedings of the IEEE/CVF Conference on Computer Vision and Pattern Recognition*, pages 3014–3023, 2021. [1](#), [2](#)
- [33] Lu Yu, Bartłomiej Twardowski, Xialei Liu, Luis Herranz, Kai Wang, Yongmei Cheng, Shangling Jui, and Joost van de Weijer. Semantic drift compensation for class-incremental learning. In *Proceedings of the IEEE/CVF conference on computer vision and pattern recognition*, pages 6982–6991, 2020. [1](#), [3](#), [7](#)
- [34] Pei Yu, Yinpeng Chen, Ying Jin, and Zicheng Liu. Improving vision transformers for incremental learning. *arXiv preprint arXiv:2112.06103*, 2021. [4](#), [7](#)
- [35] Da-Wei Zhou, Qi-Wei Wang, Han-Jia Ye, and De-Chuan Zhan. A model or 603 exemplars: Towards memory-efficient class-incremental learning. *arXiv preprint arXiv:2205.13218*, 2022. [2](#)
- [36] Fei Zhu, Xu-Yao Zhang, Chuang Wang, Fei Yin, and Cheng-Lin Liu. Prototype augmentation and self-supervision for incremental learning. In *Proceedings of the IEEE/CVF Conference on Computer Vision and Pattern Recognition*, pages 5871–5880, 2021. [1](#), [3](#), [6](#), [7](#), [8](#)
- [37] Kai Zhu, Wei Zhai, Yang Cao, Jiebo Luo, and Zheng-Jun Zha. Self-sustaining representation expansion for non-exemplar class-incremental learning. In *Proceedings of the IEEE/CVF Conference on Computer Vision and Pattern Recognition*, pages 9296–9305, 2022. [1](#), [3](#), [6](#), [7](#), [8](#)